Blood-Brain Barrier Closure Time After Controlled Ultrasound-Induced Opening Is Independent of Opening Volume

Meaghan A. O'Reilly, PhD, Olivia Hough, Kullervo Hynynen, PhD

Objectives—Microbubble-mediated focused ultrasound (US) opening of the blood-brain barrier (BBB) has shown promising results for the treatment of brain tumors and conditions such as Alzheimer disease. Practical clinical implementation of focused US treatments would aim to treat a substantial portion of the brain; thus, the safety of opening large volumes must be investigated. This study investigated whether the opened volume affects the time for the BBB to be restored after treatment.

Methods—Sprague Dawley rats (n = 5) received bilateral focused US treatments. One hemisphere received a single sonication, and the contralateral hemisphere was targeted with 4 overlapping foci. Contrast-enhanced T1-weighted magnetic resonance imaging was used to assess the integrity of the BBB at 0, 6, and 24 hours after focused US.

Results—At time 0, there was no significant difference in the mean enhancement between the single- and multi-point sonications (mean ± SD, 29.7% ± 18.4% versus 29.7% ± 24.1%; $P = .9975$). The mean cross-sectional area of the BBB opening resulting from the multi-point sonication was approximately 3.5-fold larger than that of the single-point case (14.2 ± 4.7 versus 4.1 ± 3.3 mm^2; $P < .0001$). The opened volumes in 9 of 10 hemispheres were closed by 6 hours after focused US. The remaining treatment location had substantially reduced enhancement at 6 hours and was closed by 24 hours. Histologic analysis revealed small morphologic changes associated with this location. T2-weighted images at 6 and 24 hours showed no signs of edema. T2*-weighted images obtained at 6 hours also showed no signs hemorrhage in any animal.

Conclusions—The time for the BBB to close after focused US was independent of the opening volume on the time scale investigated. No differences in treatment effects were observable by magnetic resonance imaging follow-up between larger- and smaller-volume sonications, suggesting that larger-volume BBB opening can be performed safely.

Key Words—blood-brain barrier; drug delivery; focused ultrasound

Received February 1, 2016, from the Physical Sciences Platform, Sunnybrook Research Institute, Toronto, Ontario, Canada (M.A.O., O.H., K.H.); and Department of Medical Biophysics (M.A.O., K.H.) and Institute of Biomaterials and Biomedical Engineering (K.H.), University of Toronto, Toronto, Ontario, Canada. Revised manuscript accepted for publication June 3, 2016.

We thank Shawna Rideout-Gros and Alexandra Garces for help with the animal care and preparation and Dallan McMahon for assistance with histologic assessment. Support for this work was provided by the National Institutes of Health under grant R01- EB003268, the Canada Research Chair Program, and the W. Garfield Weston Foundation.

Address correspondence to Meaghan A. O'Reilly, PhD, Sunnybrook Research Institute, 2075 Bayview Ave, C736a, Toronto, ON M4N 3M5, Canada.

E-mail: moreilly@sri.utoronto.ca

Abbreviations
BBB, blood-brain barrier; MRI, magnetic resonance imaging; US, ultrasound

doi:10.7863/ultra.16.02005

Focused ultrasound (US)-mediated opening of the blood-brain barrier (BBB) has shown promising preclinical results for the treatment of brain diseases. When combined with focused US, circulating micrometer-scale intravascular US contrast agents, or microbubbles, interact with the US field to stimulate a transient opening of the BBB and allow delivery of drug,[1–4] gene,[5–7] and cellular therapies,[8,9]

which are normally prevented from reaching the brain tissue. Numerous investigations in tumor models have shown the focused US-induced BBB opening enhances delivery of anticancer agents and improves tumor control.[10–15] In one study using multiple repeated treatments with liposomal doxorubicin, complete tumor eradication was seen in some tumor-bearing rats.[14] Recently, there has also been strong interest in the use of focused US alone for the treatment of Alzheimer disease. Prior studies have shown that focused US alone reduces the plaque burden in Alzheimer disease model mice, possibly by facilitating the delivery of endogenous antibodies.[16–18] After repeated focused US treatments, an improvement in memory in mice with Alzheimer disease was reported[17] and independently confirmed.[18]

Because the BBB plays a critical role in regulating the brain environment, rapid restoration of the BBB after treatment is important.[19] The effective time for the BBB to be restored after focused US treatment depends on the size of the agent being delivered,[20] but when acoustic parameters are chosen to avoid damage, it can occur in less than 12 hours.[20–22] However, one group reported substantially longer times for BBB closure after focused US (up to 3–5 days), with the time to close directly proportional to the disrupted volume.[23,24] In these studies, larger opening volumes were generated by using higher pressures or larger microbubble diameters. Restoration of the BBB beginning at the periphery was reported,[23] which is consistent with a reduced effect in this area due to the pressure profile of the focal spot. We hypothesize that if the opening volume is modulated by using multiple overlapping foci, which is an accepted treatment scheme that effectively flattens the exposure profile of a treatment region, the time for the BBB to close will become independent of the opening volume. Although the safety of volume opening of the BBB using multiple foci has been investigated, including in nonhuman primates,[25] the relative time to closure of these volumes compared to single-point sonications has not been investigated. Since many clinical treatments would require large-volume opening of the BBB, this factor is an important consideration for clinical translation. In this study, we tested our hypothesis in a rodent model.

Materials and Methods

Animal Preparation

All animal experiments were approved by the institutional Animal Care Committee. Male Sprague Dawley rats (n = 5; ≈300 g) were used in this study. Anesthesia was induced with oxygen and 5% isoflurane and then maintained at 2% isoflurane. The hair was removed from each animal's head with an electric razor and depilatory cream, and a 22-gauge angiocath was inserted in the tail vein. The experimental setup and single- versus multi-point sonication schemes are illustrated in Figure 1.

The animals were placed supine on a sled above a 3-axis positioning system,[26] which was used to mechanically steer the transducer focus. The sled was designed to move between the positioning system, holding the US transducer, and the bore of a 7-T MRI system (BioSpec 70/30 USR; Bruker, Billerica, MA) for treatment guidance. The animals' heads were acoustically coupled to the transducer via a water pack, which was integrated

Figure 1. a, Experimental setup. **b**, Multi-point scheme. Multiple overlapping points (gray) are used to increase the opening volume instead of a single high-pressure sonication (black). FUS indicates focused US.

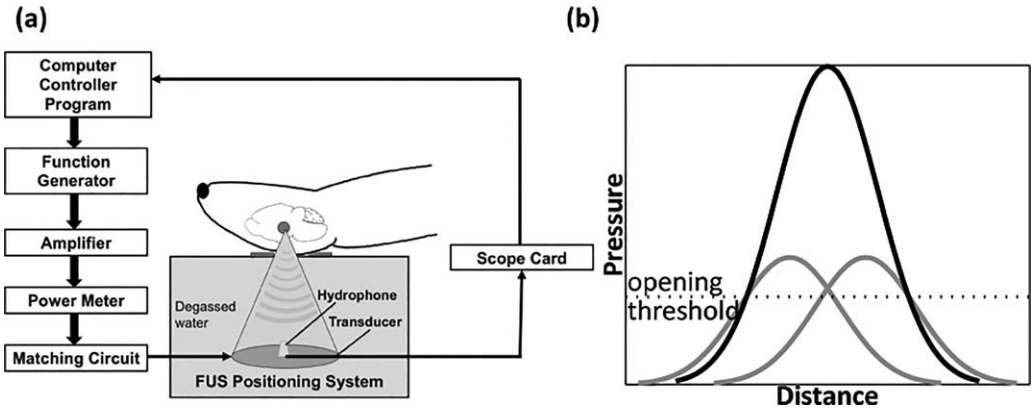

into the supporting sled, and a water bath filled with degassed, deionized water containing the transducer.

Ultrasound Exposures

The US was generated from an in-house–assembled lead zirconate titanate transducer (lead zirconate titanate from DeL Piezo Specialties, LLC, West Palm Beach, FL), with a 75-mm diameter and 60-mm focal length (focal number, 0.8). The full-width at half-maximum focal zone of the transducer was approximately 3 mm laterally and 20 mm axially. The transducer was matched to 50 Ω, 0° at its fundamental frequency (551.5 kHz), by an external matching circuit. The transducer was driven by a function generator (33220A; Agilent Technologies, Santa Clara, CA) and a radiofrequency amplifier (NP2519; NP Technology, Newbury Park, CA). Each sonication consisted of 10-millisecond bursts at a 1-Hz pulse repetition frequency for a total of 2 minutes. Sonications were applied transcranially. Pressure estimates reported in this article were based on the calibration of the transducer in water using a fiber-optic hydrophone (Precision Acoustics, Ltd, Dorchester, England) and were derated to account for the losses through the skull bone[27] and through 5 mm of brain tissue, taking the attenuation coefficient in the brain as approximately 5 Np/m/MHz.[28]

An intravenous injection of Definity microbubbles (0.02 mL/kg; Lantheus Medical Imaging, North Billerica, MA) was given, starting simultaneously with the start of the sonications. The injections were administered as a 1-minute infusion by an infusion pump (NanoJetXF magnetic resonance imaging [MRI]-compatible syringe pump; Chemyx, Stafford, TX). A custom-built polyvinylidene difluoride hydrophone[29] was used to detect microbubble emissions during the bursts. The hydrophone signal was captured to a personal computer via a scope card (ATS460; AlazarTech, Pointe-Claire, Quebec, Canada) after each burst and sampled at 20 MHz, and the frequency content of the signal was analyzed. As previously described,[30] the burst pressure was modulated on the basis of the appearance of ultraharmonic signals (1.5 and 2.5 f_0) via a real-time control algorithm implemented in C++. After each burst in a sonication, the captured signal was analyzed. The signal spectrum was integrated over a ±180-Hz band around each of 1.5 and 2.5 f_0. An increase in the signal in either of these bands to 3.5 times that at baseline (time 0) was interpreted as an ultraharmonic event. The threshold (3.5 times) was empirically chosen on the basis of the minimum change to effectively detect a signal over baseline noise with our receiver. The pressure was increased after each burst, starting from approximately 0.09 MPa in situ in steps of 6 kPa until ultraharmonic signals were detected, and then decreased to 50% of the pressure reached at detection and maintained for the remainder of the sonication. In our previous work in rats, the exposures reached peak negative pressures (in situ) of 0.28 ± 0.05 MPa (0.39 ± 0.07 MPa in water).[30] This sonication scheme is designed to ensure sufficient bubble activity to cause opening while avoiding damage associated with inertial cavitation.[30]

In each animal, one hemisphere was sonicated at a single point, and the contralateral hemisphere was treated with a 4-point overlapping grid (1.5-mm spacing). The 4-point sonication was performed by interleaving sonications during the 1-second repetition time and independently controlling the exposures at each point. The order of the sonications (single versus multi point) in each animal was randomized to avoid bias. For each animal, the sonications in each hemisphere were performed at least 5 minutes apart to allow most of the microbubbles from the previous injection to clear (half-life, ≈1.3 minutes; Definity product insert).

Magnetic Resonance Imaging

Magnetic resonance imaging was used for targeting and assessment of BBB integrity or damage. The MRI parameters are summarized in Table 1. Contrast-enhanced (0.1-mL/kg Gadovist; Bayer HealthCare Pharmaceuticals, Inc, Leverkusen, Germany) T1-weighted imaging was used to assess the integrity of the BBB immediately after focused US (time 0) as well as at

Table 1. Magnetic Resonance Imaging Parameters

Parameter	T1w	T2w	T2*w
Sequence type	RARE	RARE	GEFC
Echo time, ms	10	70	19.9
Repetition time, ms	500	4000	438.83
RARE factor	2	10	NA
Averages	3	2	1
Field of view, mm	50 × 50	50 × 50	50 × 50
Matrix	150 × 150	200 × 200	256 × 256
Slice thickness, mm	1.5	1.5	1.5

GEFC indicates gradient echo with flow compensation; NA, not applicable; RARE, rapid acquisition with relaxation enhancement; T2w, T2-weighted; and T2*w, T2*-weighted.

6 and 24 hours after focused US. The contrast agent was given as an intravenous bolus. T2-weighted imaging was used at 6 and 24 hours to detect edema. T2*-weighted images were obtained at 6 hours to assess hemorrhage.

Data Analysis

All data analysis was performed in MATLAB (The MathWorks, Natick, MA). For each animal and time point, the BBB opening was analyzed over 4 slices. An area was deemed "open" if the signal intensity exceeded the background by greater than 2 SDs. The cross-sectional area of the opening was estimated by plotting the spatial profile across the region of enhancement and measuring the dimensions of the region where the intensity exceeded the background by greater than 2 SDs.

The percentage of enhancement was measured by comparing the mean intensity in a 3×3-voxel region of interest overlapping the peak intensity to an adjacent reference region. For the hemispheres treated with multi-point sonications, the intensity was measured around each of the 4 targets making up the larger volume and averaged over the hemisphere.

The mean area of opening and mean enhancement were compared between hemispheres (single versus multi point) for 4 slices in each of the 5 animals by a 2-tailed paired *t* test. The errors on all reported means are standard deviations.

Histologic Analysis

The animals were euthanized after the 24-hour imaging follow-up. The animals were deeply anesthetized and then transcardially perfused with saline, followed by 10% neutral-buffered formalin. Two brains underwent histologic processing. After routine processing and paraffin wax embedding, the brains were axially sectioned; 5-μm-thick axial sections were cut at 300-μm intervals and stained with hematoxylin-eosin. The sonicated region was localized on hematoxylin-eosin by comparing the histologic slices with the corresponding MR images and using common landmarks (eg, midline and ventricles) for reference.

Results

Blood-brain barrier opening was achieved at all targeted sites, although 1 multi-point sonication was performed twice after a technical error prevented BBB opening from being initially achieved. T1-weighted imaging revealed that 9 of 10 hemispheres were fully closed by 6 hours after focused US (Figure 2). The remaining hemisphere was fully closed by 24 hours.

The pressure and enhancement data are illustrated in Figure 3. An unpaired *t* test showed no difference in the peak pressure achieved during the sonications in the single- versus multi-point hemispheres (0.29 ± 0.03 versus 0.30 ± 0.04 MPa; $P = .69$). In 1 sonication, a software crash at the termination of the sonication prevented the treatment pressures from being recorded, and these data were thus not included in the pressure analysis. Similarly, there was no difference in the mean enhancement observed between hemispheres at time 0 ($29.7\% \pm 18.4\%$ versus $29.7\% \pm 24.1\%$; paired *t* test: $P = .9975$).

However, the time 0 cross-sectional area of the multi-point opening was found to be approximately 3.5 times larger than that of the single point (14.2 ± 4.7 versus 4.1 ± 3.3 mm^2; paired *t* test: $P < .0001$). Example spatial profiles of the opened regions are shown in Figure 4. The multi-point profile is slightly asymmetric because the exposures were independently controlled at each of the constituent targets.

At 6 hours, the enhancement in the animal with residual BBB opening was 12% on the slice where opening could be detected and had an opening cross-sectional area of 0.8 mm^2. Follow-up T2- and T2*-weighted imaging showed no indicators of edema or hemorrhage in any of the animals, including the animal with residual BBB opening at 6 hours after focused US (Figure 5). However, histologic analysis revealed changes in the animal in which the opening persisted past 6 hours (Figure 6). A small ischemic lesion was observed in this animal. This region corresponded with the location of the T1 signal seen at 6 hours. This effect was not observed on adjacent sections (± 300 μm). Analysis of the hydrophone data for this sonication showed a small ultraharmonic signal at 29 seconds that was below the trigger threshold of the control algorithm, followed by a larger triggered event at 33 seconds (Figure 6). This target had the highest T1 enhancement of any of the sonications at time 0 (86%) but below-average peak pressure (0.28 MPa). No abnormalities were seen in the surrounding region, where closure occurred within 6 hours, in the contralateral hemisphere, or in the other processed brain. Extravasated red blood cells were not observed in either brain.

Discussion

In this study, we sought to examine the effect of the volume of opening on the time for the BBB to close. Our results suggest that the time for the BBB to close after the sonication is independent of the opening volume when the pressure and volume are decoupled. Previous studies in which a larger opening volume was associated with higher pressures have shown the BBB being restored beginning at the periphery of the disrupted zone.[23] We have overcome this factor by using multiple overlapping foci to flatten the exposure profile. Taken in context with prior studies on BBB closure,[21,23,24,28] this approach supports variations in closing time, for a given tracer or therapeutic agent, as related to the exposure level and degree of effect on the tissue.

In this study, we used ultraharmonic emissions to control the treatment exposures. As the driving pressure is increased, microbubbles become more nonlinear, first emitting harmonic signals, followed by subharmonic and ultraharmonic signals at higher exposures, and finally broadband emissions.[31] Others have correlated an increase in harmonic emissions, signifying stable cavitation, with successful BBB opening[32,33] and the presence of broadband emissions, indicating inertial cavitation, with damage.[32] Although harmonic signals can arise from tissue nonlinearities, subharmonic and ultraharmonic emissions are bubble specific, and as they occur

Figure 2. a, Magnetic resonance images from 2 animals at 0, 6, and 24 hours. Arrows indicate openings. The lower panel shows an animal with a residual opening at 6 hours. **b**, Treated sites showing opening as a function of time after focused US (FUS).

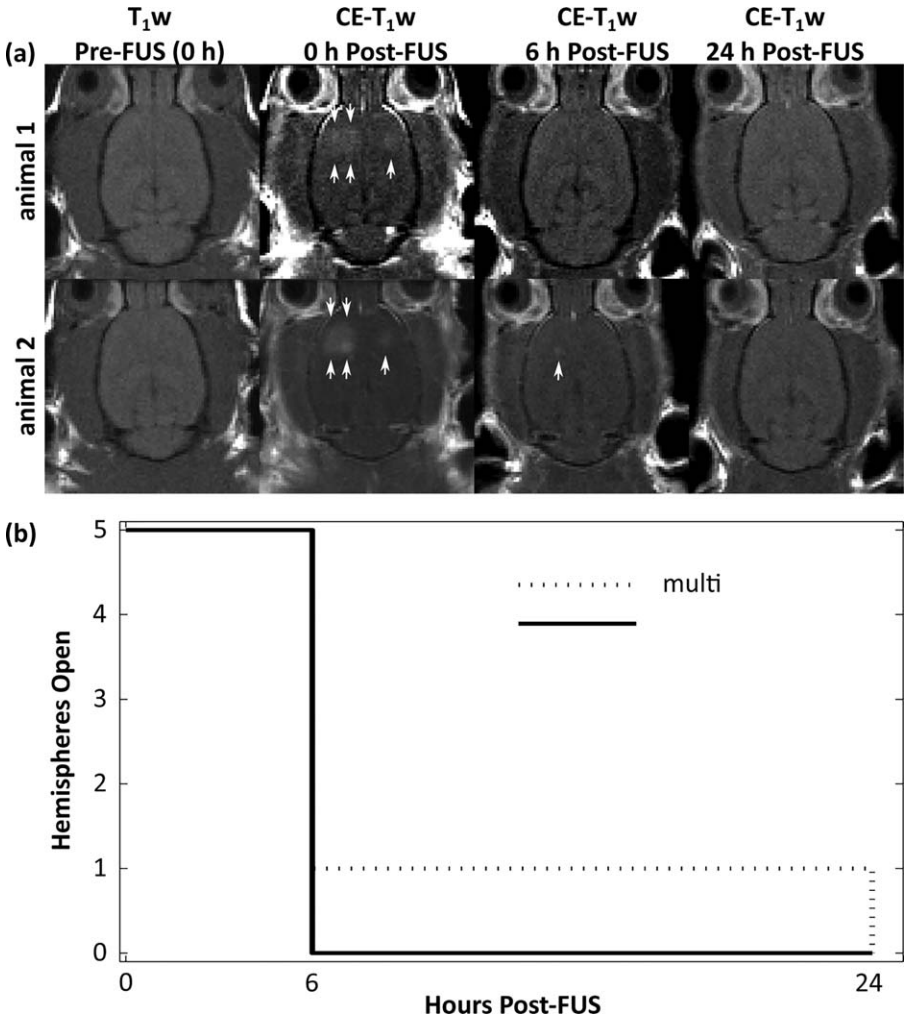

at pressures below the inertial cavitation threshold, we use them to mark an upper safety threshold. In this specific implementation, we have used the first 2 ultraharmonics instead of the subharmonic because of the susceptibility of the subharmonic band to equipment noise in our particular setup. The type of tissue damage observed in the 1 case in this study was not seen in our prior work using the real-time treatment controller,[30] although we previously observed some red blood cell extravasation at the 2-hour time point, which was not seen here. The lesion was small (diameter, ≈0.4 mm) and confined to a single histologic slice (slice thickness, 5 μm; distance between slices, 300 μm), and if present, such an effect may have been too small for detection in earlier studies. This effect might also have been missed in the prior study because of the differences in the time points for tissue collection (24 hours versus 2 hours or 7 days). However, small differences also exist in the controller scheme, which could be contributing factors. For example, in the prior work, single-point sonications were used with a 2-Hz pulse repetition frequency. Here we have used multi-point interleaved sonications and thus reduced the per-point pulse repetition frequency to 1 Hz to allow our treatment system to cycle through all of the points within the repetition time. With this approach, the pressure increment between bursts doubled from our prior study, and potentially, this step size is too large. In the hydrophone data, we also

Figure 3. a, Mean peak pressures achieved during the sonication for the multi- and single-point sonications ($P = .67$). **b**, Mean enhancement at time 0 for the multi- and single-point sonications ($P = .9975$).

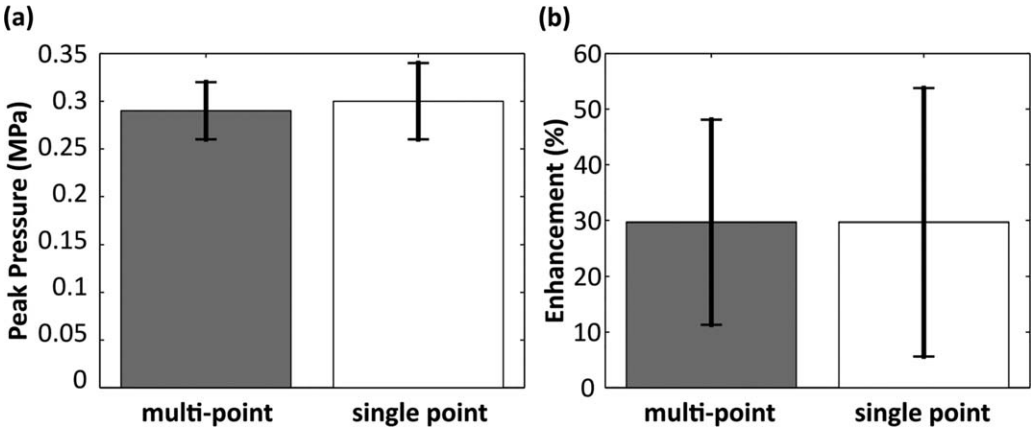

Figure 4. a, Mean cross-sectional areas for the multi- and single-point sonications ($P < .0001$). **b**, Example spatial profile for multi- and single-point disrupted regions.

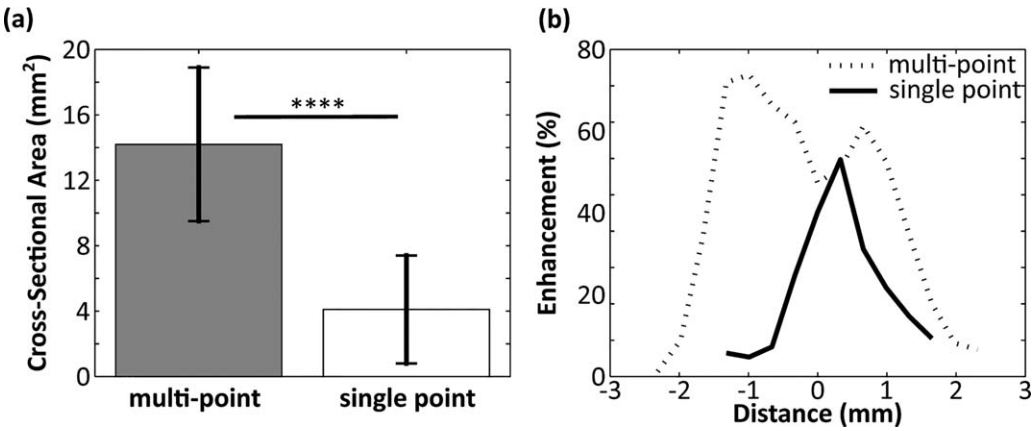

Figure 5. T2-weighted (T2w) and T2*-weighted (T2*w) images showing no indicators of edema or hemorrhage in the animal with persistent BBB opening at 6 hours. The hypointense regions seen in the T2-weighted image are artifacts due to air in the ear canals of the rat. FUS indicates focused US.

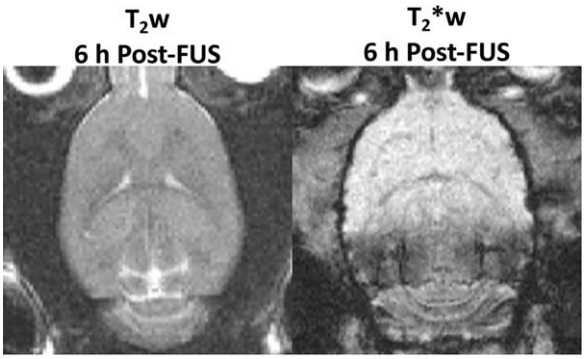

observed that during this sonication, ultraharmonic signal components were present but did not satisfy the threshold criteria to register as an event in the control algorithm. To date, we have used a static detection threshold, which was determined empirically based on the goal of keeping a minimum threshold value while avoiding false-positive results due to noise. A dynamic threshold based on the standard deviation of the baseline noise across several reference sonications might provide a more robust approach that could prevent important events from being missed. Furthermore, combining our methods with those proposed by others using the harmonic emissions for control[34] may prove the most robust.

As with our previous study with this control method,[30] our results show wide variations in the enhancement levels

Figure 6. a, Histologic (hematoxylin-eosin) section from the animal in which an opening was observed at 6 hours, showing a small region of injury (arrow). The surrounding tissue, where closure occurred within 6 hours, is unaffected. **b**, Fast Fourier transform (FFT) at time 29 and 33 seconds for the sonication corresponding to the damage; a.u. indicates arbitrary units. **c**, Area under the FFT in the 1.5 and 2.5 f_0 frequency bands as a function of time.

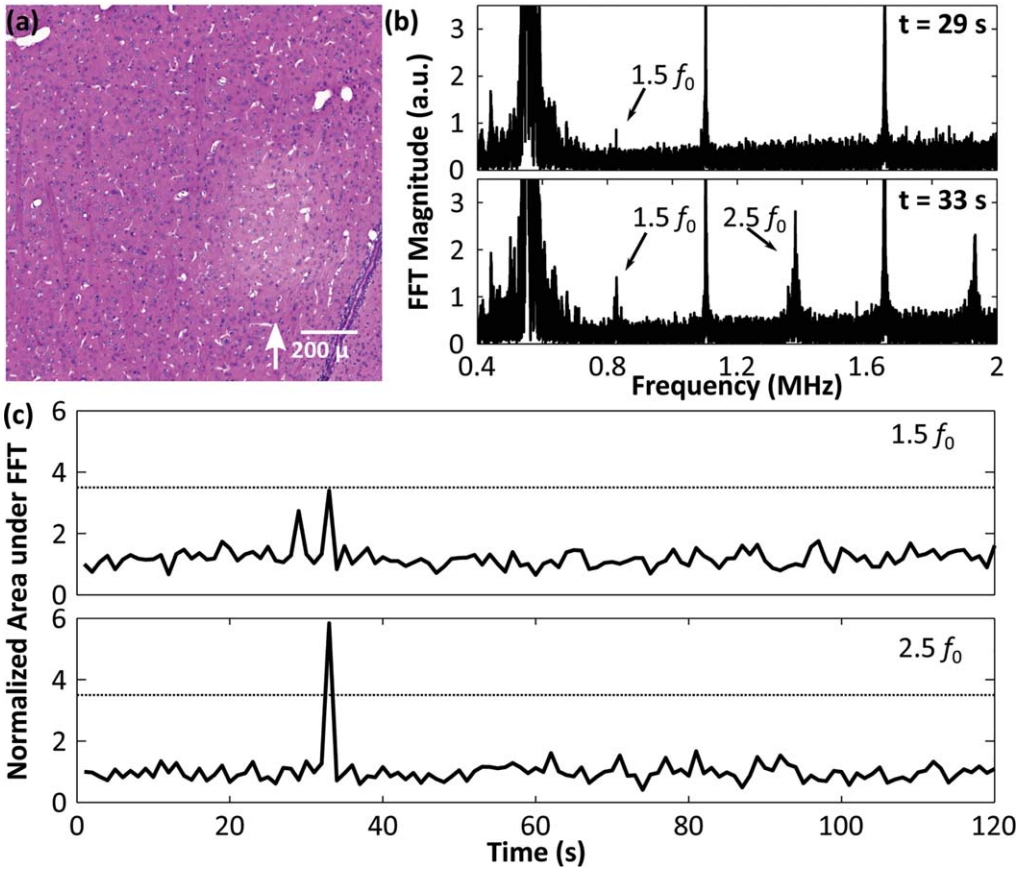

between animals. This technique controls the bubble behavior but may not account for variability due to the bubble concentration or biological response. Future work should investigate these parameters.

Some differences exist between this study and the published works[23,24] that motivated our study. The most important is the use of overlapping foci to create the larger volume, as described in the introduction. Additionally, the species differed (rat versus mouse), as did the US frequency and sonication scheme. In our study, we chose to use 0.5 MHz because of its clinical relevance and larger focal spot size. One limitation of our study was that it was performed at a single frequency, and we cannot do an exact comparison with studies that use substantially higher or lower frequencies. Our slice thickness on the MR images was 3 times that used by Samiotaki et al[23,24]; thus, some small effects may have been averaged out. However, in the first study by Samiotaki et al,[23] the delayed opening that was observed could be seen to extend through most of the brain, exceeding our slice thickness.

The most notable difference in the two studies is the delivery of the MRI contrast agent. In this study, we used the recommended clinical dose of 0.1 mmoL/kg, delivered intravenously. Samiotaki et al[23,24] used an intraperitoneal injection of the contrast agent to delay the contrast peak and allow for improved longitudinal imaging. However, the intraperitoneal dose was 60 times the dose in our study, potentially providing greater sensitivity to small changes in the barrier integrity, but that approach might have limited clinical relevance. Finally, in the second study of Samiotaki et al,[24] a 50 times higher dose of Definity was used than in our study. It should also be noted that when Definity microbubbles were used,[24] the reported time to close for some sonication parameters (<8 hours) was more comparable with that reported here.

Other limitations of this study should be noted. The group size used here was small. Additionally, with the exception of 1 sonication, the barrier was closed by the first follow-up time point. Thus, small differences may exist between the multi- and single-point sonications within the 6-hour window after focused US.

The closure time of the BBB after opening is not the only safety consideration for clinical translation, but our results complement existing behavioral and cognitive studies that have considered the safety of this approach in mice[35] and primates.[25,36] The time for the BBB to close after focused US is independent of the opening volume when multiple overlapping foci are used. No differences in the treatment effect were observable by MRI follow-up between larger- and smaller-volume sonications, which suggests that larger-volume focused US BBB opening does not present additional safety risks. These findings have important implications for clinical implementation of this method and the ability to safely treat therapeutically relevant tissue volumes.

References

1. Fan CH, Ting CY, Liu HL, et al. Antiangiogenic-targeting drug-loaded microbubbles combined with focused ultrasound for glioma treatment. *Biomaterials* 2013; 34:2142–2155.
2. Ting CY, Fan CH, Liu HL, et al. Concurrent blood-brain barrier opening and local drug delivery using drug-carrying microbubbles and focused ultrasound for brain glioma treatment. *Biomaterials* 2012; 33: 704–712.
3. Kinoshita M, McDannold N, Jolesz FA, Hynynen K. Noninvasive localized delivery of Herceptin to the mouse brain by MRI-guided focused ultrasound-induced blood-brain barrier disruption. *Proc Natl Acad Sci USA* 2006; 103:11719–11723.
4. Kinoshita M, McDannold N, Jolesz FA, Hynynen K. Targeted delivery of antibodies through the blood-brain barrier by MRI-guided focused ultrasound. *Biochem Biophys Res Commun* 2006; 340:1085–1090.
5. Thévenot E, Jordão JF, O'Reilly MA, et al. Targeted delivery of self-complementary adeno-associated virus serotype 9 to the brain, using magnetic resonance imaging–guided focused ultrasound. *Hum Gene Ther* 2012; 23:1144–1155.
6. Huang Q, Deng J, Wang F, et al. Targeted gene delivery to the mouse brain by MRI-guided focused ultrasound-induced blood-brain barrier disruption. *Exp Neurol* 2012; 233:350–356.
7. Huang Q, Deng J, Xie Z, et al. Effective gene transfer into central nervous system following ultrasound-microbubbles-induced opening of the blood-brain barrier. *Ultrasound Med Biol* 2012; 38:1234–1243.
8. Burgess A, Ayala-Grosso CA, Ganguly M, Jordão JF, Aubert I, Hynynen K. Targeted delivery of neural stem cells to the brain using MRI-guided focused ultrasound to disrupt the blood-brain barrier. *PLoS One* 2011; 6:e27877.
9. Alkins RC, Burgess A, Ganguly M, et al. Focused ultrasound delivers targeted immune cells to metastatic brain tumors. *Cancer Res* 2013; 73:1892–1899.
10. Liu HL, Hua MY, Chen PY, et al. Blood-brain barrier disruption with focused ultrasound enhances delivery of chemotherapeutic drugs for glioblastoma treatment. *Radiology* 2010; 255:415–425.
11. Liu HL, Hua MY, Yang HW, et al. Magnetic resonance monitoring of focused ultrasound magnetic nanoparticle targeting delivery of

therapeutic agents to the brain. *Proc Natl Acad Sci USA* 2010; 107: 15205–15210.

12. Chen PY, Liu HL, Hua MY, et al. Novel magnetic ultrasound focusing system enhances nanoparticle drug delivery for glioma treatment. *Neuro Oncol* 2010; 12:1050–1060.
13. Treat LH, McDannold N, Zhang Y, Vykhodtseva N, Hynynen K. Improved anti-tumor effect of liposomal doxorubicin after targeted blood-brain barrier disruption by MRI-guided focused ultrasound in rat glioma. *Ultrasound Med Biol* 2012; 38:1716–1725.
14. Aryal M, Vykhodtseva N, Zhang YZ, Park J, McDannold N. Multiple treatments with liposomal doxorubicin and ultrasound-induced disruption of blood-tumor and blood-brain barriers improve outcomes in a rat glioma model. *J Control Release* 2013; 169:103–111.
15. Wei KC, Chu PC, Wang HYJ, et al. Focused ultrasound-induced blood-brain barrier opening to enhance temozolomide delivery for glioblastoma treatment: a preclinical study. *PLoS One* 2013; 8:e58995.
16. Jordão JF, Thévenot E, Markham-Coultes K, et al. Amyloid-β plaque reduction, endogenous antibody delivery and glial activation by brain-targeted, transcranial focused ultrasound. *Exp Neurol* 2013; 248:16–29.
17. Burgess A, Dubey S, Yeung S, et al. Alzheimer disease in a mouse model: MR imaging–guided focused ultrasound targeted to the hippocampus opens the blood-brain barrier and improves pathologic abnormalities and behavior. *Radiology* 2014; 273:736–745.
18. Leinenga G, Götz J. Scanning ultrasound removes amyloid-β and restores memory in an Alzheimer's disease mouse model. *Sci Transl Med* 2015; 7:278ra33.
19. Abbott NJ, Rönnbäck L, Hansson E. Astrocyte-endothelial interactions at the blood-brain barrier. *Nat Rev Neurosci* 2006; 7:41–53.
20. Marty B, Larrat B, Landeghem MV, et al. Dynamic study of blood-brain barrier closure after its disruption using ultrasound: a quantitative analysis. *J Cereb Blood Flow Metab* 2012; 32:1948–1958.
21. Mei J, Cheng Y, Song Y, et al. Experimental study on targeted methotrexate delivery to the rabbit brain via magnetic resonance imaging–guided focused ultrasound. *J Ultrasound Med* 2009; 28:871–880.
22. Hynynen K, McDannold N, Vykhodtseva N, et al. Focal disruption of the blood-brain barrier due to 260-kHz ultrasound bursts: a method for molecular imaging and targeted drug delivery. *J Neurosurg* 2006; 105:445–454.
23. Samiotaki G, Vlachos F, Tung YS, Konofagou EE. A quantitative pressure and microbubble-size dependence study of focused ultrasound-induced blood-brain barrier opening reversibility in vivo using MRI. *Magn Reson Med* 2012; 67:769–777.
24. Samiotaki G, Konofagou EE. Dependence of the reversibility of focused- ultrasound-induced blood-brain barrier opening on pressure and pulse length in vivo. *IEEE Trans Ultrason Ferroelectr Freq Control* 2013; 60:2257–2265.
25. McDannold N, Arvanitis CD, Vykhodtseva N, Livingstone MS. Temporary disruption of the blood-brain barrier by use of ultrasound and microbubbles: safety and efficacy evaluation in rhesus macaques. *Cancer Res* 2012; 72:3652–3663.
26. Ellens NPK, Kobelevskiy I, Chau A, et al. The targeting accuracy of a preclinical MRI-guided focused ultrasound system. *Med Phys* 2015; 42:430–439.
27. O'Reilly MA, Muller A, Hynynen K. Ultrasound insertion loss of rat parietal bone appears to be proportional to animal mass at submegahertz frequencies. *Ultrasound Med Biol* 2011; 37:1930–1937.
28. Hynynen K, McDannold N, Vykhodtseva N, Jolesz FA. Noninvasive MR imaging–guided focal opening of the blood-brain barrier in rabbits. *Radiology* 2001; 220:640–646.
29. O'Reilly MA, Hynynen K. A PVDF receiver for ultrasound monitoring of transcranial focused ultrasound therapy. *IEEE Trans Biomed Eng* 2010; 57:2286–2294.
30. O'Reilly MA, Hynynen K. Blood-brain barrier: real-time feedback-controlled focused ultrasound disruption by using an acoustic emissions-based controller. *Radiology* 2012; 263:96–106.
31. Neppiras EA. Acoustic cavitation. *Phys Rep* 1980; 61:159–251.
32. McDannold N, Vykhodtseva N, Hynynen K. Targeted disruption of the blood-brain barrier with focused ultrasound: association with cavitation activity. *Phys Med Biol* 2006; 51:793–807.
33. Tung YS, Vlachos F, Choi JJ, Deffieux T, Selert K, Konofagou EE. In vivo transcranial cavitation threshold detection during ultrasound-induced blood-brain barrier opening in mice. *Phys Med Biol* 2010; 55: 6141–6155.
34. Arvanitis CD, Livingstone MS, Vykhodtseva N, McDannold N. Controlled ultrasound-induced blood-brain barrier disruption using passive acoustic emissions monitoring. *PLoS One* 2012; 7:e45783.
35. Howles GP, Bing KF, Qi Y, Rosenzweig SJ, Nightingale KR, Johnson GA. Contrast-enhanced in vivo magnetic resonance microscopy of the mouse brain enabled by noninvasive opening of the blood-brain barrier with ultrasound. *Magn Reson Med* 2010; 64:995–1004.
36. Downs ME, Buch A, Karakatsani ME, Konofagou EE, Ferrera VP. Blood-brain barrier opening in behaving non-human primates via focused ultrasound with systemically administered microbubbles. *Sci Rep* 2015; 5:15076.